MODELING OF SULFIDE MICROENVIRONMENTS ON MARS. S. P. Schwenzer[1], J. C. Bridges[2], A. McAdam[3], E. D. Steer[1], P. G. Conrad[3], S. P. Kelley[1], R. C. Wiens[4], N. Mangold[5], J. Grotzinger[6], J. L. Eigenbrode[3], H. B. Franz[3], and B. Sutter[7], [1]The Open University, Milton Keynes MK7 6AA, UK; susanne.schwenzer@open.ac.uk; [2]University of Leicester LE1 7RH, UK; [3]NASA Goddard Space Flight Center, Greenbelt, MD, USA; [4]Los Alamos National Laboratory, Los Alamos, NM 87544, USA; [5]Laboratoire Planétologie et Géodynamique de Nantes, LPGN/CNRS UMR6112, 44322 Nantes, France ; [6]Division of Geological and Planetary Sciences, California Institute of Technology, Pasadena, CA, USA; [7]NASA/JSC, Houston TX 77058, USA.

Yellowknife Bay (YKB; sol 124-198) is the second site that the Mars Science Laboratory Rover Curiosity investigated in detail on its mission in Gale Crater. YKB represents lake bed sediments from an overall neutral pH, low salinity environment [1], with a mineralogical composition which includes Ca-sulfates, Fe oxide/hydroxides, Fe-sulfides, amorphous material, and trioctahedral phyllosilicates [2]. We investigate whether sulfide alteration could be associated with ancient habitable microenvironments in the Gale mudstones. Some textural evidence for such alteration may be present in the nodules present in the mudstone [Fig. 1A].

Alteration and fluid chemistry: We carried out thermochemical modelling [3-5], concluding that incongruent dissolution under low temperature (10 °C) diagenetic conditions of the precursor host rock was the most likely alteration pathway to form the YKB mudstone secondary assemblage. The succession of events leading to the observed mudstones and the Ca-sulfate veins was modelled as follows [3-5]: An incoming groundwater caused incongruent dissolution of the precursor rock, with a dissolved composition consisting of 70 % amorphous material as found in Portage soil (assumed to be volcanic or impact glass), with additional olivine and dissolved 'host rock'. The model indicates clay formation and a resultant brine enriched in Ca and S sufficient to form Ca-sulfate veins, but also carrying additional components, e.g., silica [3]. Because the Ca-sulfate veins are pure sulfate veins with very little SiO_2, Ba and other elements, we propose that an initial deposition of the majority of dissolved solids led to a 'dirty' Ca-sulfate deposit, which was buried, subsequently dissolved and the Ca-sulfate re-deposited in the veins [4,5]. While these models explain the final conditions in the sediment, here we also explore inhomogeneities, especially the presence of sulfides, the question of whether they cause an acidic environment or not, and finally the presence of carbonate.

CheMin and SAM measurements: CheMin x-ray diffraction analyses detected 1 % pyrrhotite and traces of pyrite in the YKB mudstones [2], alongside with akaganeite, which is an alteration product of pyrrhotite at its terrestrial type location. The presence of magnetite and hematite (if in equilibrium and not detrital remnants) constrain the redox conditions at mildy oxidiz-

ing. Akaganeite, bassanite, and phyllosilicates contribute to the H_2O release, and minor carbonates (abundances below the CheMin detection limit) and sulfides are candidates for some of the CO_2 and SO_2 releases detected during SAM pyrolysis, respectively [6].

Methods: We use the CHIM-XPT software [7] to model alteration conditions of sulfide grains within host rocks at Gale crater, using titration models (see [3]). For the model presented here we added various amounts of pyrite and siderite to the host rock compositions used in [3], which we deduced from the Portage soil components [9-11] The model temperature is 10 °C. As an analog for those microenvironments, sulfide weathering in an L chondrite weathered in Antarctica was examined by EMPA and SEM analysis (see [12]).

Microenvironments: To investigate microenvironments that might occur around detrital sulfide grains, we modeled alteration of a mixture of 55 % Portage soil [11] with 22 % olivine [2], 17 % pyrite and 6 % siderite with the fluid that evaporates in the veins [4,5]. This mixture represents a general basaltic rock environment with dominantly olivine dissolution in the close vicinity of a sulphide grain. Siderite as the
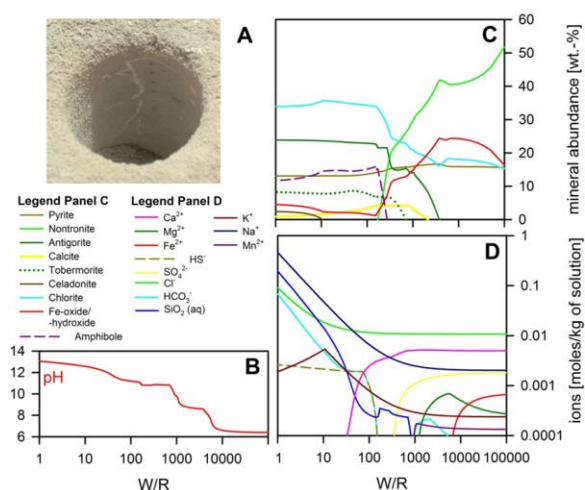

Fig. 1. Potential microenvironment around a pyrite grain in carbonate-bearing Portage-composition sediment. (A) Curiosity observation of the Sheepbed structure in the Cumberland Drill Hole, (B) pH at various W/R. Note that the system is buffered at various stages (stepped nature of the plot). (C) Alteration mineral assemblage for a range of W/R. Note that especially at high W/R nontronite, Fe-hydroxide and chlorite dominate. (D) Fluid composition W/R.

carbonate phase is found in martian rock compositions (i.e., the Lafayette, Nakhla, Governador Valadares meteorites, [13]), and part of the CO_2 evolution from Portage soil during SAM analysis was consistent with minor siderite [14]. In the model it serves to enhance CO_2 partial pressure during reactions that might precipitate the CO_2 from the starting fluid thus lowering CO_2-partial pressure in the system. Siderite does not cause other changes in the overall rock composition, since Fe is one of the most abundant cations. SAM results suggest possible carbonate in the Sheepbed mudstone [6]. Our microenvironment model considers the alteration of a pyrite grain inside Portage-composition sediments via the fluid that is derived from the sulfate-rich deposits and enhanced CO_2 partial pressure [4,5].

The reaction of the model composition at 10 °C results in a pH increase with increasing dissolution (Fig. 1B), and a nontronite–Fe-hydroxide–chlorite assemblage at high W/R, followed by a chlorite–antigorite–pyrite assemblage at low W/R (Fig. 1C). The re-precipitation of pyrite, as predicted by the model (Fig. 1C) is likely, if the system is reducing. If there is an oxidizing agent (potentially perchlorate [15]) oxidized S-bearing phases could precipitate instead. If entirely rock-controlled, the redox balance of the fluid changes from SO_4^{2-}-dominated at high W/R to HS^--dominated at low W/R (Fig. 1D). Because such microenvironments are of spatially restricted nature, and – assuming the pyrite dissolution occurs contemporaneously with the fluid movement into the fractures that become sulfate veins – the dynamic nature of the water flow environment would have resulted in fluid recharge events that would have kept W/R high, therefore nontronite–hematite formation appears likely.

The SO_4^{2-}/HS^--changes in the fluid (Fig. 1D) towards lower W/R, which is a result of this rock-dominated system. In the presence of an oxidant, sulfate would dominate in solution and precipitate. The carbonate assumed to be present in this microenvironment stays in solution, but buffers the pH (Fig. 1B), and thus could contribute to the stabilization of microenvironmental conditions. Finally, Fe-hydroxide precipitation occurs (alongside nontronite and chlorite), which could explain the nodule formation without dominating the ChemCam analyses. However, at no point in the model does the entire system become acidic. The rock buffering capacity is stonger than the amount of pyrite dissolution in the case presented here.

Microenvironments in Antarctic Meteorites:

To examine the spatial extent of sulfide controlled acidic micro-environments, areas of sulfide weathering in Antarctic L chondrite QUE 94214 were studied [16]. Sulfide weathering is characterized by enhanced silicate weathering including etch pits when compared to areas of typical Antarctic weathering, which is highly oxidizing [17,18]. Secondary minerals formed in these acidic micro-environments are restricted to thin films of Fe-oxyhydroxides in fractures and along grain boundaries and very small (<50 μm) in-situ pockets of smectites in pyroxenes and olivines. Primary minerals displayed significant dissolution through pitting and stripping along cleavage planes. Decreases in Si, Mg, Mn are accompanied by an increase of Fe in the olivine and pyroxene crystals within 1 mm of weathering sulfide grains. Areas of abundant pitting are raised by up to 3 wt.% FeO. This Fe increase is concentrated in imperfections within the crystals in grain boundaries and so nanophase Fe-oxyhydroxides are inferred to have been deposited at these boundaries. SiO_2 measured in alteration products in these areas is higher than the average SiO_2 content in alteration products throughout the sample (with SiO_2 4-6 wt%) and so the material stripped from the ferromagnesian minerals does not appear to have been transported far. These observations demonstrate the small spatial distribution of sulfide induced enhanced alteration haloes in low-water and low-temperature environments.

Conclusions: The overall conditions in the rock are buffered by the main mineral reactions causing neutral to alkaline environments despite the presence of dissolving sulphides. The sulfide grains are associated with very localised acid alteration, as observed in the L-chondrites in microscopic detail, where sulfide alteration causes halos of etching and Fe-oxide deposition. Similar localized chemical and pH gradients could have formed the nodules observed in YKB (Fig. 1A). Together the circumneutral overall rock alteration and the chemical gradients towards sulfide grains would have offered a variety of redox and pH conditions, including chemical gradients favourable for habitability.

References: [1] Grotzinger, J. P. et al. (2014) *Science, 343,* DOI: 10.1126/science.1242777. [2] Vaniman, D. T. et al. (2014) *Science, 343,* DOI: 10.1126/science. 1243480. [3] Bridges, J. C. et al. (2015) *JGR,* DOI:10.1002/2014JE004757. [4] Schwenzer S. P. et al. (2015) 46th *LPSC,* Abstract #1441. [5] Schwenzer, S. P. et al. (in rev.) Fluids During Diagenesis and Sulfate Vein Formation in Sediments at Gale Crater, Mars, *MAPS.* [6] Ming, D. W. et al. (2014) Science, 343, DOI: 10.1126/science.1245267. [8] Reed, M. H. et al. (2010) User Guide for CHIM-XPT. University of Oregon, Eugene, Oregon. [9] Morris, R. V. et al. (2013) 44th LPSC, abstr. #1653. [10] Morris, R. V. et al. (2014) 45th LPSC, abstr. #1319. [11] Gellert, R. et al. (2013) 44th LPSC, abstr. #1432. [12] Steer, E. D. et al. (2015) 46th LPSC, abstr. #1820. [13] Bridges, J.C. et al. (2001) *Space Sci. Rev.*, 96, 365–392.. [14] Sutter, B. et al. (2015) AGU fall meeting, abstr. P31F-07. [15] Glavin, D. P. et al. (2013) J. Geophys. Res. Planets, 118, 1955–1973. [16] Steer, E. D. (2016) PhD thesis, The Open University. [17] Gooding, J. L. (1981) LPSC XII, abstr. p. 350-351. [18] Lee, M. R. & Bland, P. A. (2004) *GCA, 68*: 893–916.